# CHAPTER IV

RESULTS AND DISCUSSION

4.1 γ-Ray Irradiation Effects on Chitosan Properties

4.1.1 Molecular Weight of γ-Ray Irradiated Chitosan

Chitosan starting materials with the degree of deacetylation of 70% and 90% were used. Both types of chitosan were irradiated with ^{60}Co γ-rays in water at various doses. Generally, natural chitosan resources are organic-inorganic hybrid materials. Thus, even controlling the extraction and purification processes to avoid the mineral contamination, $CaCO_3$ and other inorganic salts are still in the product. In the present work, the materials used gave ash contents about 0.09 to 0.32%, implying the high purity.

Wenwei *et al.* (1993) reported that the non-acetylated moiety of chitosan is more sensitive to γ-ray irradiation than the acetylated moiety.

Ershov *et al.* (1987) suggested a degradation mechanism of amino group in γ-ray irradiated chitosan (Scheme 4.1). It was found that amino group could be converted to be ammonia, as a result, strong hydrogen bonding in chitosan reduced after γ-ray irradiation.

$$R\text{-}NH_2 \; + \; H\bullet \; \longrightarrow \; R\bullet(C_2) \; + \; NH_3$$
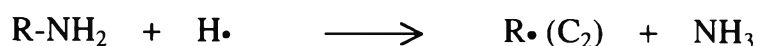
Scheme 4.1 Degradation of amino group in γ-ray irradiated chitosan.

Table 4.1 Intrinsic viscosity and molecular weight of chitosan samples (70% DD and 90% DD) before and after γ-ray irradiation.

Dose / kGy	70% DD		90% DD	
	[η]	MW	[η]	MW
0	479.69±15	996419±896	339.18±14	412162±814
20	268.53±10	590347±440	278.46±6	251283±258
40	185.87±17	425926±979	207.55±3	181366±154
60	140.84±11	329817±460	143.37±1	120232±62
80	110.04±9	263279±332	127.07±1	105171±67
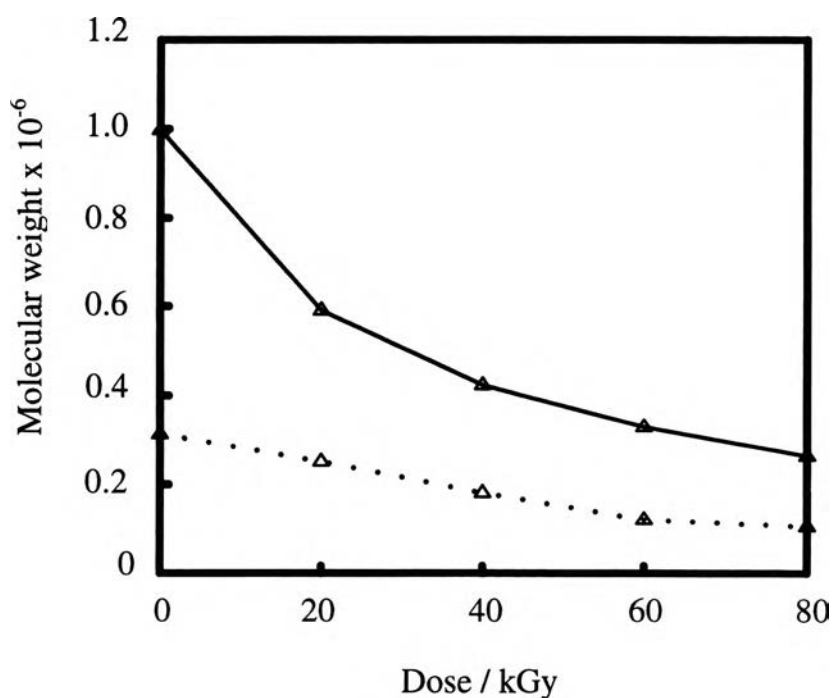
Figure 4.1 Molecular weight of chitosan samples before and after γ-ray irradiation, (a)) -Δ- : 70% DD, and (b) ··Δ·· : 90% DD.

Table 4.1 and Figure 4.1 show that the molecular weights of chitosan samples (70% and 90% DD) are decreased with an increasing in γ-ray dose. The decrease in molecular weight was significant at starting of irradiation to γ-ray dose of 40 kGy. It should be noted that 70% DD chitosan performed the decrease more obviously than that of 90% DD. This might be due to the fact that 70% DD chitosan contains low amino group content leading to the few hydrogen bonding network and few closed packing portions compared to that of 90% DD chitosan. As a result, the lower degree of deacetylation chitosan has more portions that can be destroyed by γ-ray irradiation than the higher degree of deacetylation chitosan.

Theoretically, the molecular weight could either be increased by polymerization process or decrease by degradation process. In the present work, after γ-ray irradiation, the products obtained were found to be dissolved completely in dilute acetic acid solution. This implied that the crosslinking did not occur. As a result, the γ-ray irradiation might bring chain degradation prior to chain combination.

4.1.2 Chemical Structure of γ-Ray Irradiated Chitosan

FT-IR (KBr, cm^{-1}): 3422 (O-H stretching), 2881 (C-H stretching), 1655 (C=O amide I), 1596 (C=O amide II), 1153 (bridge oxygen stretching), 1079 and 1032 (C-O stretching), and 896 (pyranose ring).

Figure 4.2 shows the characteristic peaks of the products after γ-ray irradiation. The four major peaks, i.e., in the range of 1153 cm^{-1} referred to (1-4) oxygen bridge, 1079 and 1032 cm^{-1} referred to C-O-C, and

896 cm^{-1} referred to pyranose ring, were found to be remained in the chitosan structure. This implied that the γ-ray dose up to 80 kGy did not destroy the main structure of chitosan.
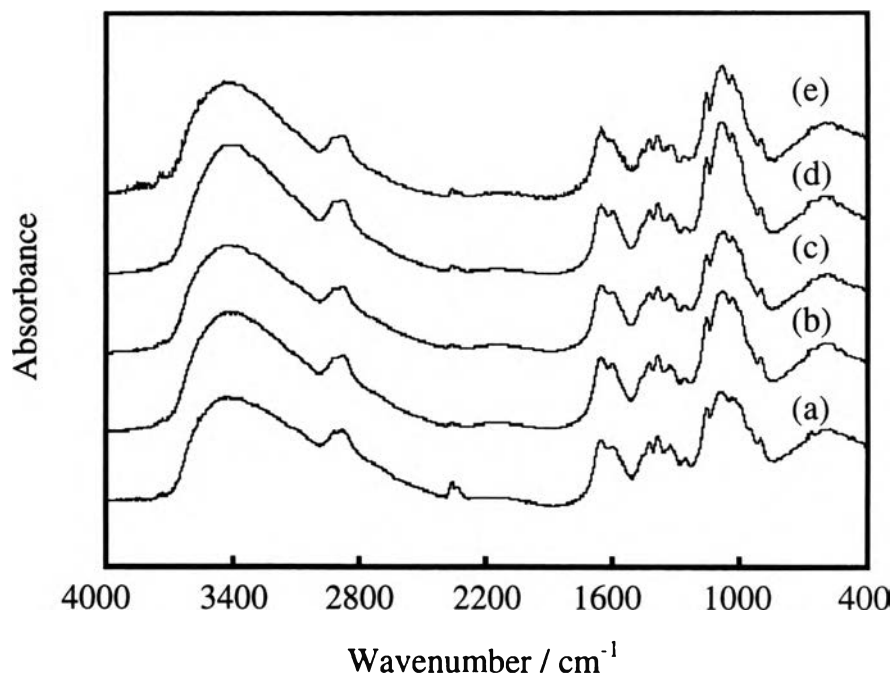

Figure 4.2 FT-IR spectra of (a) chitosan samples (90% DD), and after γ-ray irradiation for (b) 20, (c) 40, (d) 60, and (e) 80 kGy.

After γ–ray irradiation, the product obtained was dissolved in 0.04 M acetic acid solution in order to study the structural changing by UV spectroscopy. Figure 4.3 shows the increases in peak absorption at 227 and 290 nm. This might be due to the formation of carbonyl and carboxyl groups as reported by Ulanski and Rosiak (1992). The possibilities of these generated end groups reported by Ulanski and Rosiak (1992) are summarized in Scheme 4.2.
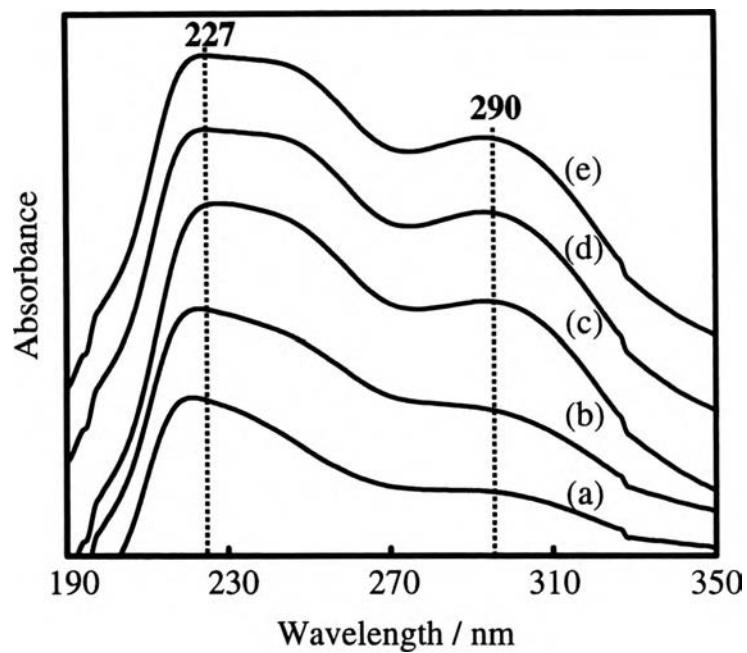
Figure 4.3 UV spectra of chitosan (90% DD) in 0.04 M acetic acid solution, (a) before, and after γ-ray irradiation for (b) 20, (c) 40, (d) 60, and (e) 80 kGy.
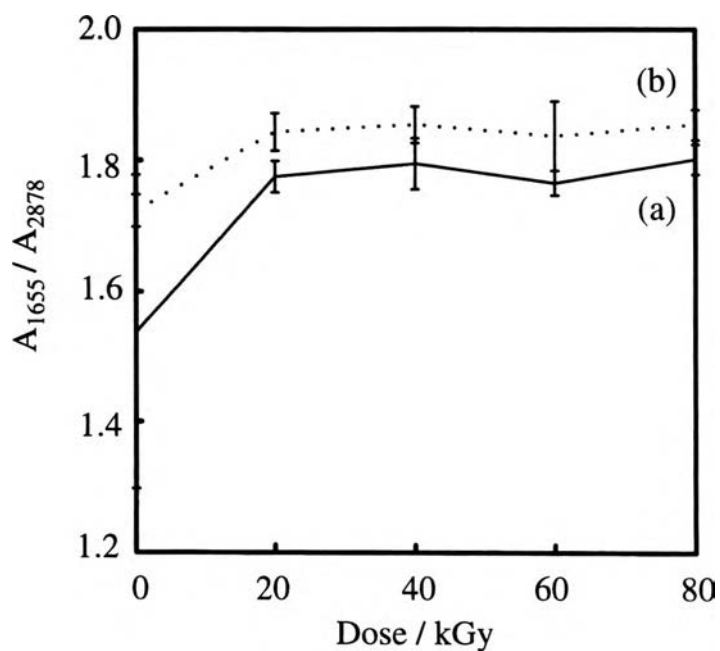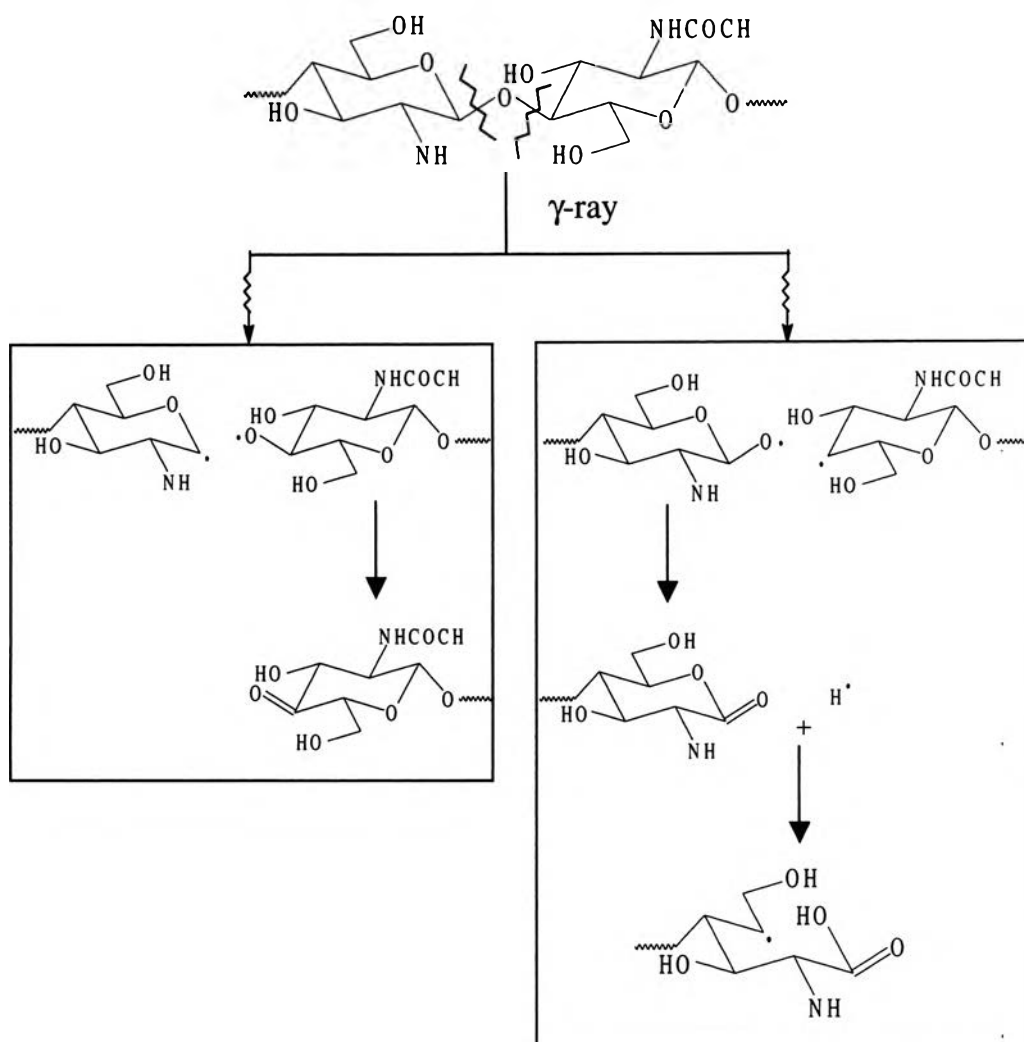

Figure 4.4 Absorbance ratio of amide I band and C-H stretching band of chitosan in the case of, (a) 70% DD, and (b) 90% DD.

Scheme 4.2 Mechanisms of carbonyl and carboxyl formations of γ–ray irradiated chitosan (Ulanski and Rosiak, 1992).

After γ-ray irradiation, the radicals were formed on the chitosan chain. The decomposition of these radicals, then, caused the formation of carbonyl and carboxyl end groups. Taking the FT-IR patterns (Figure 4.2) into the consideration, it might be concluded that the chain degradation might occur at a low level and the main structure of chitosan was maintained.

4.1.3 Degree of Deacetylation of γ-Ray Irradiated Chitosan

Degree of deacetylation of chitosan samples before and after irradiation might be changed as an effect of γ-ray. The amide I band at 1655 cm^{-1} referred to *N*-acetyl group content and the methylene band at 2881 cm^{-1} as an internal standard were used for quantitative analysis by FT-IR technique. Figure 4.4 shows that the absorbance ratio after γ-ray irradiation is almost constant even the amount of γ-ray increased. This implied that the chain scission by γ-ray irradiation was occurred at random position. It should be noted that Yoksan *et al.* (2000) reported the similar results about the unchanged % DD after γ-ray irradiation. Thus, it can be concluded that degree of deacetylation is not affected after γ-ray irradiation.

4.1.4 Thermal Stability of γ-Ray Irradiated Chitosan

Figure 4.5 shows the weight loss at 52.26°C followed by the second peak at 309.62°C, which can also be seen as two endothermic peaks in DTA. The former decay reveals the loss of moisture and water contents in chitosan sample. The latter peak shows the degradation of chitosan, which might be owing to the breakage of glucosidic bond between pyranose rings. The degradation temperatures of chitosan before and after γ-ray irradiation were not much different even increasing the amount of γ-ray (Figure 4.6).

The results correspond with that of Yoksan *et al.* (2000) for the case of γ-ray irradiation on dry flake chitosan. In general, in the case of semi crystalline polymer, the crystalline portion controls the thermal stability, especially the degradation. Although the studies by DSC is further required
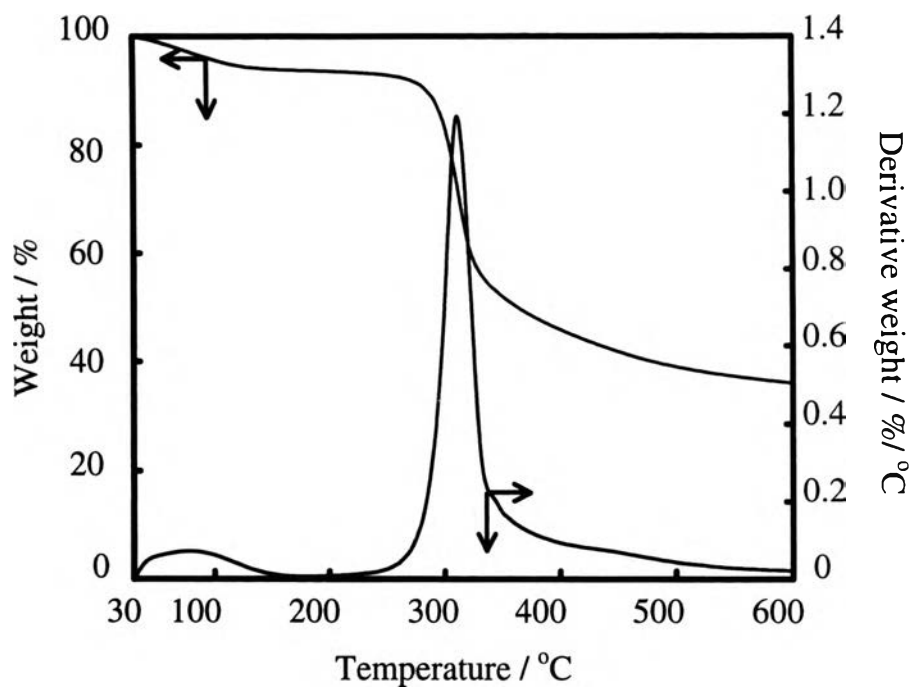
Figure 4.5 TG/DTA of chitosan samples with 90% DD after γ-ray irradiation for 20 kGy.
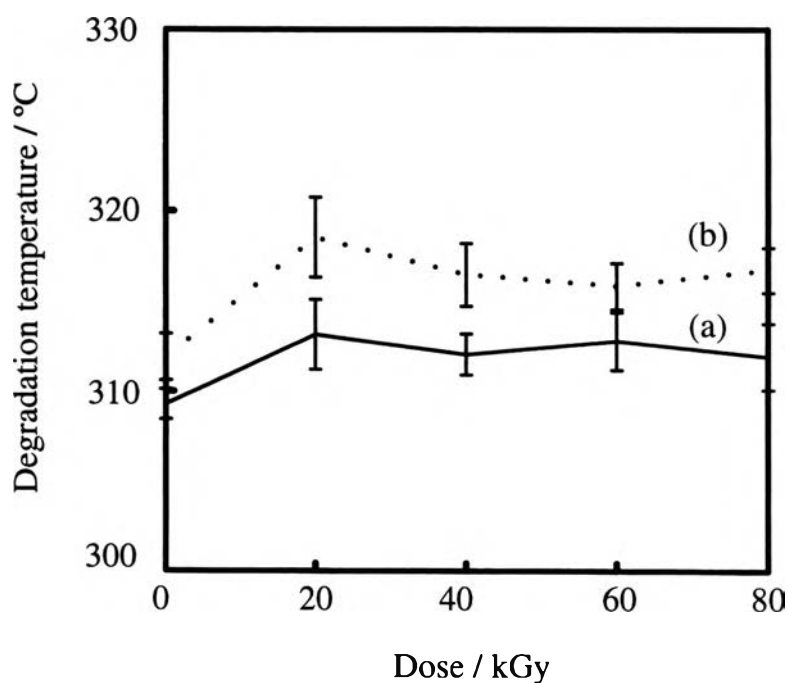

Figure 4.6 Degradation temperature of chitosan samples after γ-ray irradiation, (a) 70% DD, and (b) 90% DD.

to confirm the heat required to degrade the γ-ray irradiated chitosan, at present, it might be concluded that the rigid crystalline portion remained. The thermal stability was still controlled by the undestroyed rigid crystalline part.

4.1.5 Morphology of γ-ray Irradiated Chitosan

After γ-ray irradiation, the appearance of flake-like chitosan was changed to powder-like. Figure 4.7 shows the XRD patterns of chitosan having the specific peaks at 10.39° and 19.82°. After γ-ray irradiation, the peaks become broader. This implied the amorphous region generated after irradiation. However, after the γ-ray dose was above 40 kGy, the XRD patterns of γ-ray irradiated chitosan did not change. Taking thermal stability results into the consideration, the γ-ray irradiation might induce the amorphous portion to a certain level. The rigid crystalline part might be packed tightly with hydrogen bonding (Goosen, 1997). As a result, above 40 kGy of irradiation, the XRD patterns were still remained. Scheme 4.3 summarized a model that the energy of γ-ray can destroy the loose packing portion, however, the solid packing still remains even at high dose level.
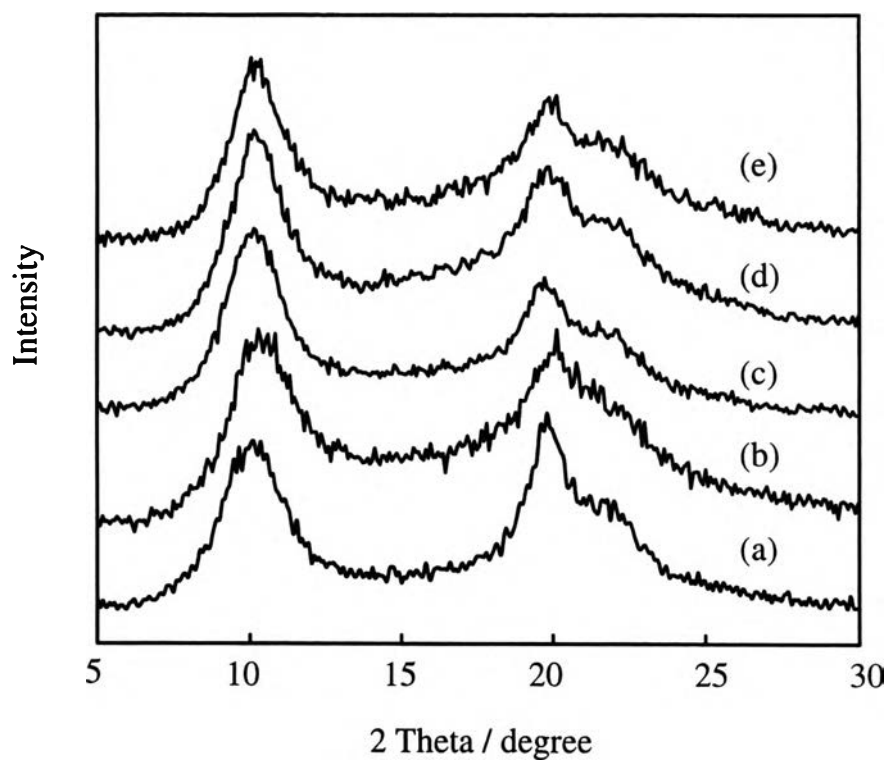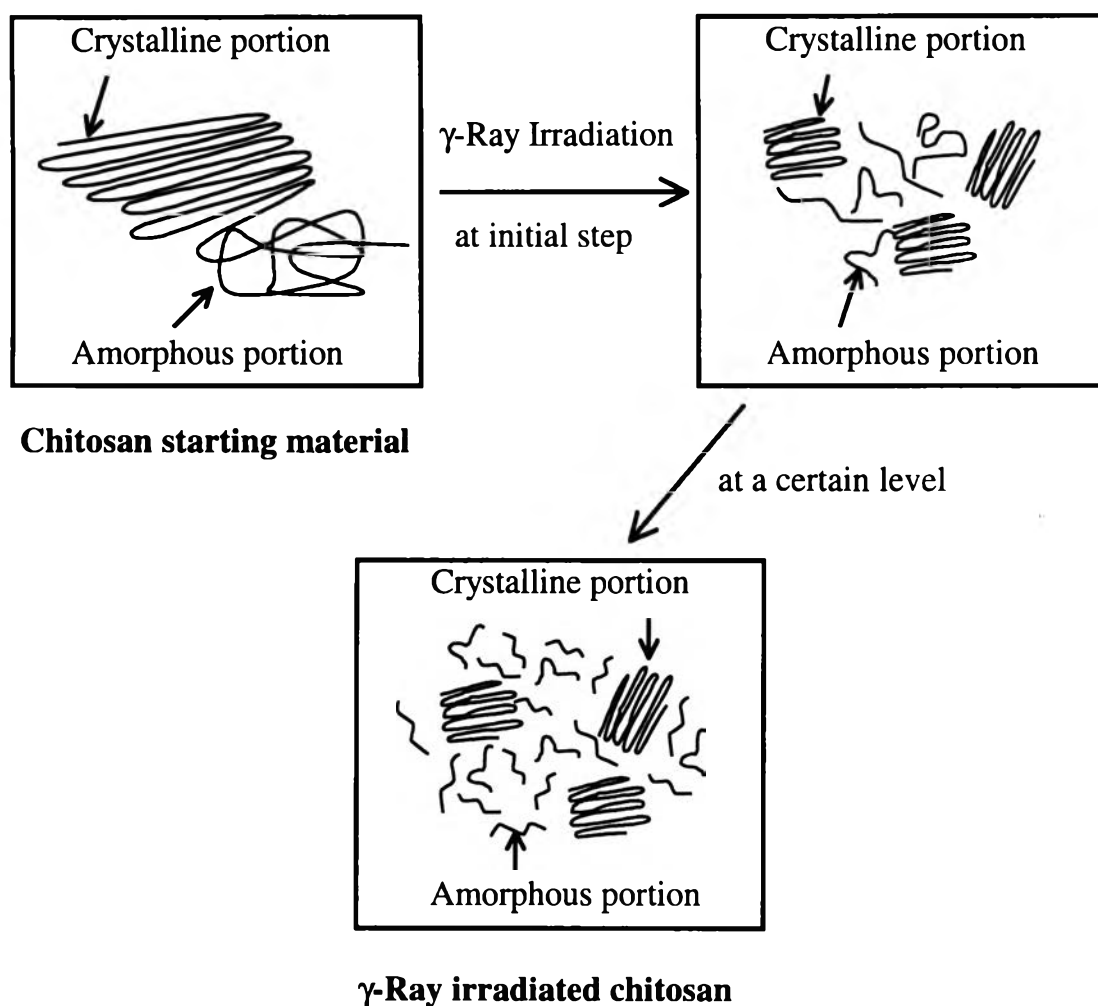
Figure 4.7 XRD patterns of chitosan samples (90% DD) (a) before, and after γ-ray irradiation for (b) 20, (c) 40, (d) 60, and (e) 80 kGy.

Crystalline portion		Crystalline portion
	γ-Ray Irradiation	
	at initial step	
Amorphous portion		Amorphous portion

Chitosan starting material

at a certain level

Crystalline portion
Amorphous portion

γ-Ray irradiated chitosan

Scheme 4.3 Schematic draw of γ-ray effect on the morphology of chitosan.

4.2 Preparation of γ-Ray Irradiated Chitosan-Glutaraldehyde-Stearylamine (ICGS)

γ-Ray irradiated chitosan was conjugated with stearylamine at amino group by using glutaraldehyde as a spacer and followed by a reductive amination (Scheme 3.1), to obtain γ-ray irradiated chitosan-glutaraldehyde-stearylamine or ICGS. The reaction was unique as it was carried out in a salt

state, i.e., ammonium salt formed in dilute acetic acid solution, at ambient temperature within few hours.
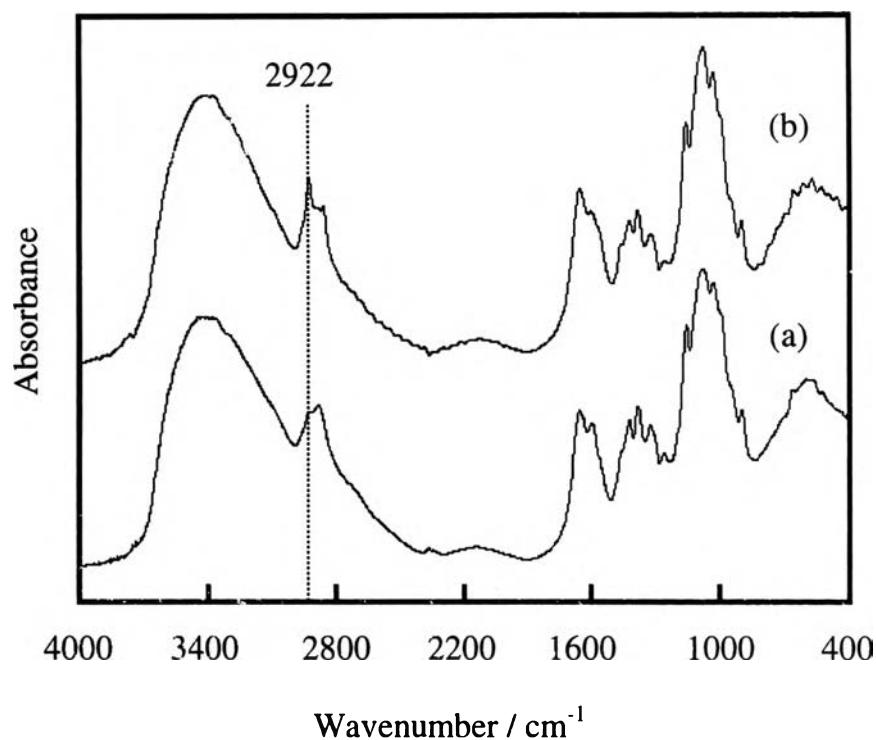

Figure 4.8 FT-IR spectra of γ-ray irradiated chitosan (90% DD at γ-ray irradiation for 20 kGy), (a) before, and (b) after hydrophobic conjugation.

FT-IR (KBr, cm^{-1}): 3422 (O-H stretching), 2922 and 2853 (C-H stretching), 1655 (C=O amide I), 1596 (C=O amide II), 1466 (C-H bending), 1153 (bridge oxygen stretching), 1079 and 1032 (C-O stretching), and 897 (pyranose ring). Figure 4.8 shows the CH stretching at 2922 cm^{-1} referred to the hydrophobic chain, which was found to be significant after the reaction proceeded. The efficiency of reaction was analyzed by quantitative FT-IR using the peak at 2922 cm^{-1} referred to methylene group and at 896 cm^{-1}

referred to pyranose ring and used as an internal standard (Figure 4.9). The absorbance ratio, in another words, %methylene groups, was found to be increased for up to 20% as the amount of dose increased. This implied that the higher the amount of dose led the higher the efficiency of reaction.
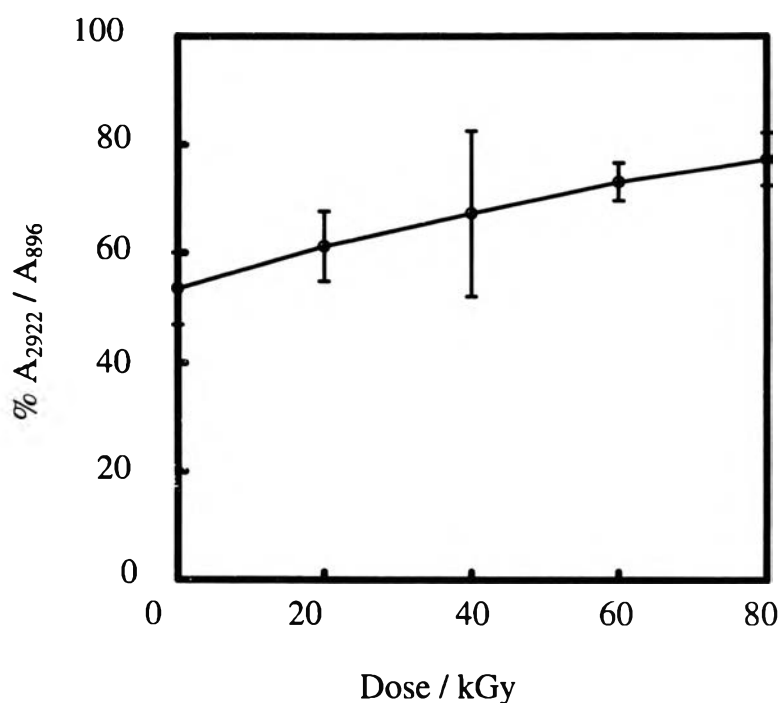

Figure 4.9 Quantitative analysis of ICGS (90% DD) at various γ-ray amounts.

In addition, the ICGS was found to be soluble in 1% (v/v) acetic acid solution but insoluble in the tested organic solvents, i.e., benzene, toluene, chloroform, dichloromethane, acetonitrile, DMSO, and pyridine.

4.2.1 Thermal Stability of ICGS

Thermal stability of ICGS with amount of dose 20 kGy is shown in Figure 4.10.
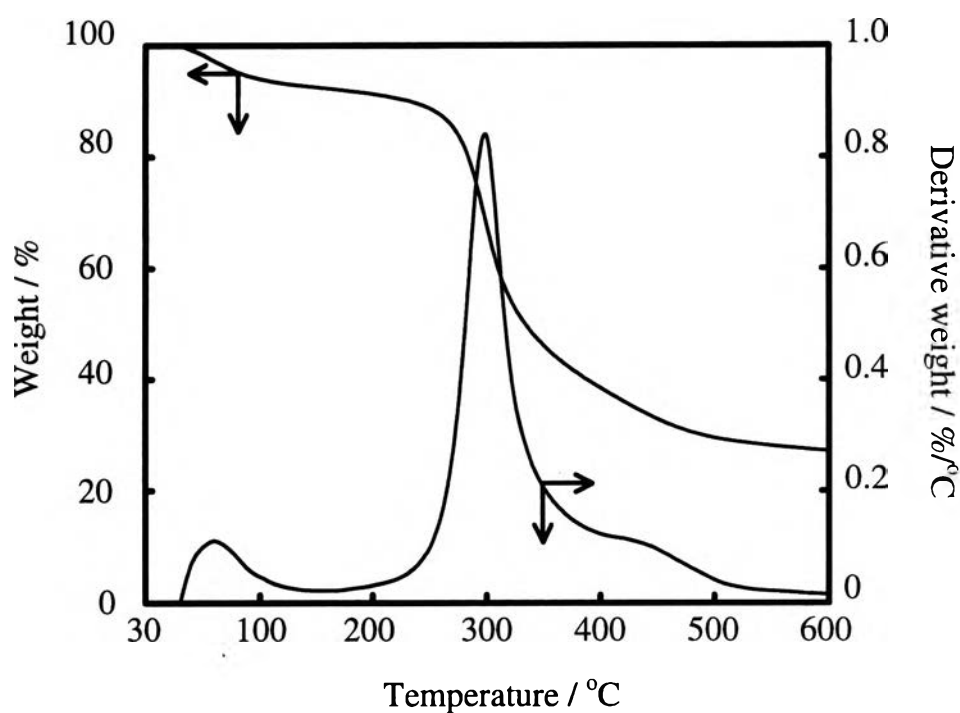

Figure 4.10 TG/DTA of ICGS with 90% DD under the γ-ray irradiation at 20 kGy.

After hydrophobic conjugation, TGA and DTA diagrams of the compound show three endothermic peaks. The weight loss at the initial step refers to the loss of moisture and water. The sharp peak at 288.97°C might be due to the breakage of the glucosidic linkage. The last peak at 428.75°C revealed the loss of stearylamine-glutaraldehyde. This implied the successful conjugation of stearylamine and glutaraldehyde onto γ-ray irradiated chitosan

chain. Comparing to that of chitosan starting material, degradation temperature of ICGS was decreased for 12°C (Figure 4.11). In another words, ICGS became more sensitive to thermal degradation than unmodified one, which might be due to the introduction of the long and bulky hydrophobic chain.
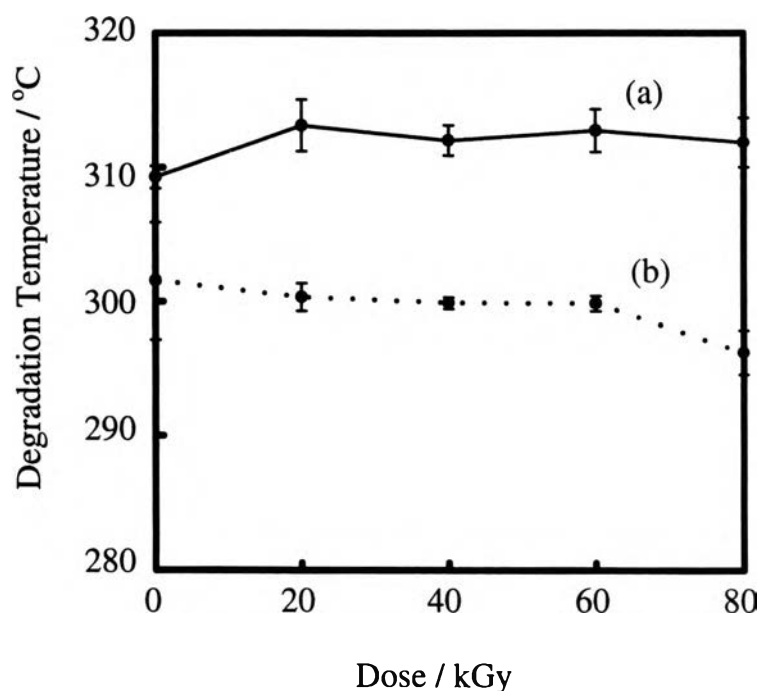

Figure 4.11 Degradation temperature of γ-ray irradiated chitosan, (a) before, and (b) after hydrophobic conjugation.

4.2.2 Morphology of ICGS

It is known that after chain modification, the packing of chitosan will be different from the original one. XRD analysis is an alternative way to observe the changing. The XRD pattern of ICGS gives only a single peak at 19.98°, while starting chitosan gives both peaks at

10.39° and 19.82° (Figure 4.12). This implied that the conjugation of the glutaraldehyde-stearylamine disturbed the packing morphology, and as a result, the amorphous portion was significantly increased.
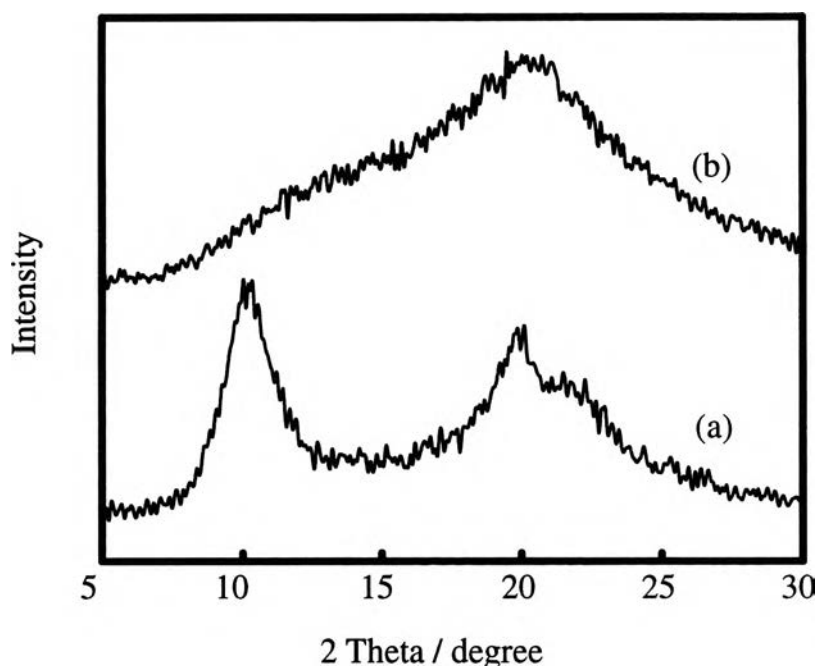

Figure 4.12 XRD patterns of γ-ray irradiated chitosan (90% DD at γ-ray 80 kGy), (a) before, and (b) after hydrophobic conjugation.

4.3 Aggregation Studies of ICGS

In order to investigate the chitosan-micelle formation, the mixture of ICGS and model drug was investigated for the hydrophilic and/or hydrophobic interactions. In the present work, chloramphenicol was used as a model drug because of the availability and chromophore that can be both qualitative and quantitative analyzed by UV-Vis spectroscopy.

Figure 4.13 shows UV spectra of the mixture between ICGS/acetic solution and chloramphenicol/ethanol at the concentration of 0.8 UV absorbance value at the peak maximum, i.e., 219 nm and 247 nm, respectively. Theoretically, when the molecular interaction occurs, the electron density and localization of each molecule will change. As a result, the auxochromic effect can be observed by UV/Vis spectroscopy. Here, the peak at 274 nm referring to carbonyl group in chloramphenicol was applied as a peak for auxochromic effect detecting group.
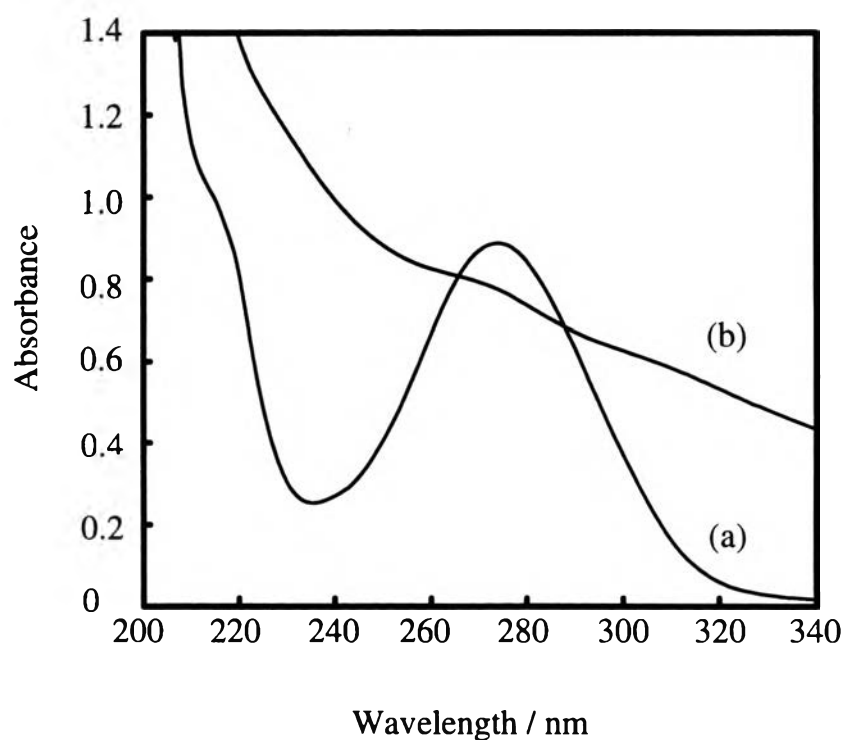

Figure 4.13 UV spectra of (a) chloramphenicol in ethanol and (b) ICGS (90% DD at γ-ray 80 kGy) in 0.04 M acetic acid solution.

The absorbances at 274 nm of the mixture of unmodified chitosan and chloramphenicol dose not show any hypochromic effect even after 2 days (Figure 4.14). In contrast, the modified chitosan showed significant hypochromic effect, especially after the mixing time for 2 days. In the other words, the hypochromic effect was occurred. This implied that electron density inside the structure of chloramphenicol was changed. As a result, the aggregation between ICGS and chloramphenicol was expected to occur by the driving force of hydrophilic and/or hydrophobic interactions (Miwa *et al.*, 1998).
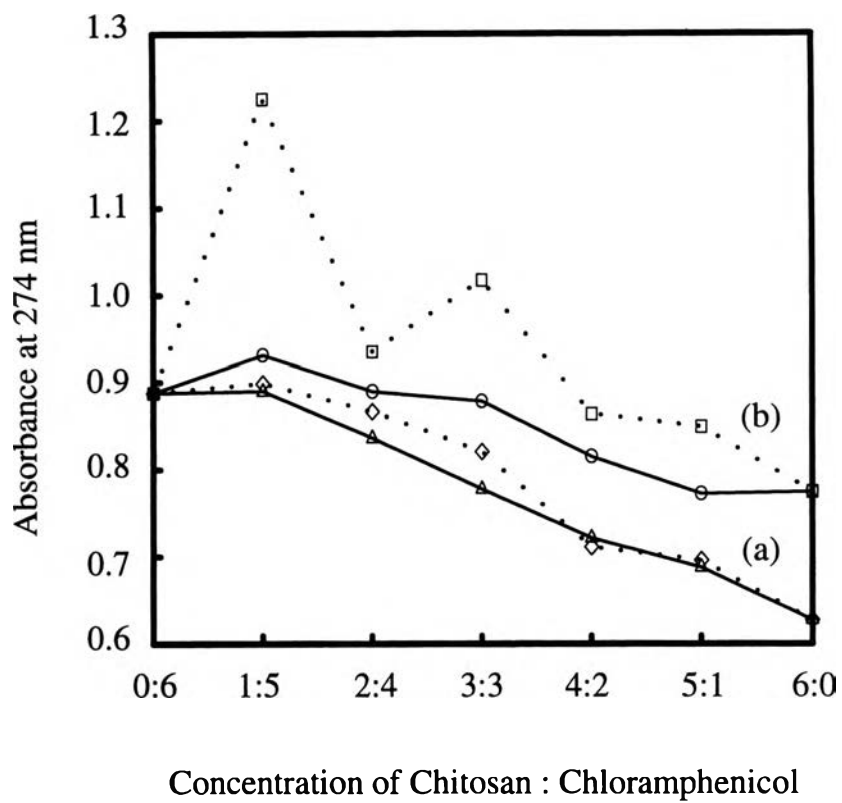
Figure 4.14 Absorbance at 274 nm for the mixture of chloramphenicol with

(a) γ-ray irradiated chitosan (90% DD, 80 kGy); -Δ- after mixing for 15 min,

-◊- after mixing for 2 days, and (b) ICGS; -o- after mixing for 15 min, and -

□- after mixing for 2 days.